Grazing function g and collimation angular acceptance

Stephen G. Peggs*
Brookhaven National Laboratory, Upton, New York 11973, USA

Valentina Previtali
CERN, Geneva, and EPFL, Lausanne, Switzerland
(Received 7 November 2008; published 2 November 2009)

The *grazing function* g is introduced—a synchrobetatron optical quantity that is analogous (and closely connected) to the Twiss and dispersion functions β, α, η, and η'. It parametrizes the rate of change of total angle with respect to synchrotron amplitude for grazing particles, which just touch the surface of an aperture when their synchrotron and betatron oscillations are simultaneously (in time) at their extreme displacements. The grazing function can be important at collimators with limited acceptance angles. For example, it is important in both modes of crystal collimation operation—in channeling and in volume reflection. The grazing function is independent of the collimator type—crystal or amorphous—but can depend strongly on its azimuthal location. The rigorous synchrobetatron condition $g = 0$ is solved, by invoking the close connection between the grazing function and the slope of the normalized dispersion. Propagation of the grazing function is described, through drifts, dipoles, and quadrupoles. Analytic expressions are developed for g in perfectly matched periodic FODO cells, and in the presence of β or η error waves. These analytic approximations are shown to be, in general, in good agreement with realistic numerical examples. The grazing function is shown to scale linearly with FODO cell bend angle, but to be independent of FODO cell length. The ideal value is $g = 0$ at the collimator, but finite nonzero values are acceptable. Practically achievable grazing functions are described and evaluated, for both amorphous and crystal primary collimators, at RHIC, the SPS (UA9), the Tevatron (T-980), and the LHC.

DOI: 10.1103/PhysRevSTAB.12.114001 PACS numbers: 41.85.−p, 29.85.Fj, 29.20.−c

I. INTRODUCTION

The *impact parameter* of a particle striking an aperture—the displacement of the particle relative to the edge of the aperture—is important in the general discussion of particle losses. For example, if a proton has an insufficiently large impact parameter when it strikes the leading edge of an amorphous collimator that is typically of order 1 m long, there is a significant probability that it will escape back into the halo of the beam via multiple scattering. In this case it is necessary to accurately model the realistic distribution of impact parameters, if the collimation efficiency and loss maps are to be accurately predicted or explained. The impact angle is also important. For example, if a proton strikes a relatively very short crystal primary collimator that is of order 5 mm long, and which is oriented for channeling or for volume reflection, then the impact angle must lie within a limited angular acceptance if collimation is to be efficient. Here, too, a realistic distribution of impact angles is important if a particular case is under quantitative study.

Diffusion mechanisms play a crucial role in determining the impact displacement and impact angle distributions, both in reality and in simulation—always assuming that injection transients have died down. It is conventional to assume—or to assert—that slow heating in transverse and/or in longitudinal phase space causes the particle amplitudes to increase slowly, so that eventually the aperture is exceeded. The rate of heating (and its dependence on the amplitudes) has a strong effect on the impact distributions, and so must be considered carefully and separately for each particular case.

This paper is concerned with a linear optical mechanism that broadens the distribution of impact angles *in the limit of no diffusion* if the optical dispersion function η and/or its slope η' is nonzero. For example, if η is significant then there is an anticorrelation between the betatron amplitude and the synchrotron amplitude of a particle that just hits the aperture after an extremely long period of extremely weak heating—one amplitude tends to be larger when the other is smaller. Such *grazing* particles all have a vanishing small "zero" impact parameter, by definition.

Several other implicit assumptions are made, besides operating *in the limit* of no diffusion, in order to make the analysis as simple and as general as possible. All transverse and longitudinal motion is assumed to be linear. There is no coupling between horizontal, vertical, and longitudinal motion, except through the dispersion function and its slope. The aperture (collimator) has zero length, a reasonable approximation for a very short crystal collimator primary. There may be significant differences if one or more of these assumptions is removed—allowing

*peggs@bnl.gov

linear coupling and nonlinear distortions, for example—but their consideration is beyond the scope of this paper.

A. The linear formalism for grazing

The total horizontal displacement x_T of a particle as it passes a collimator is the sum of its betatron and synchrotron displacements,

$$x_T = x_\beta + x_s, \tag{1}$$

where the betatron displacement and angle oscillate according to

$$x_\beta = a_x \sin(\phi_x) \tag{2}$$

$$x'_\beta = \frac{a_x}{\beta}[\cos(\phi_x) - \alpha \sin(\phi_x)]. \tag{3}$$

Here β and α are horizontal Twiss functions at the collimator, a_x is the betatron amplitude, and the betatron phase advances with turn number t according to

$$\phi_x(t) = 2\pi Q_x t + \phi_{x0}. \tag{4}$$

Similarly, the synchrotron displacement and angle are

$$x_s = \eta\delta \tag{5}$$

$$x'_s = \eta'\delta, \tag{6}$$

where $\delta = \Delta p/p$ is the relative momentum offset, which performs synchrotron oscillations according to

$$\delta = a_s \sin[\phi_s(t)] \tag{7}$$

$$= a_s \sin(2\pi Q_s t + \phi_{s0}). \tag{8}$$

Here η and η' (dispersion and its slope) are optical quantities at the collimator, complementing β and α. The total angle x'_T of a particle is thus written in general as

$$x'_T = \frac{a_x}{\beta}[\cos(\phi_x) - \alpha \sin(\phi_x)] + \eta' a_s \sin(\phi_s). \tag{9}$$

The betatron and synchrotron amplitudes a_x and a_s vary with time if any diffusion mechanisms are present. Here, in the limit of zero diffusion, we assume that the typical fractional change in a_x or a_s is very much less than one in one betatron or synchrotron period. After an extremely long time these amplitudes will have evolved so that the aperture can only just be touched. Such a *grazing particle* has a vanishing small impact parameter. It only just touches the edge of a collimator displaced by x_c when its betatron and synchrotron displacements are simultaneously in time at their extrema—either maxima or minima—such that

$$a_x + |\eta| a_s = |x_c|. \tag{10}$$

This equation correlates the betatron and synchrotron amplitudes of the set of grazing particles, since it is trivially rewritten as

$$a_x = |x_c| - |\eta| a_s. \tag{11}$$

Simultaneous betatron and synchrotron oscillation extrema are achieved on turn number t when the phases are

$$\phi_x(t) = \quad \mathrm{sgn}(x_c) \qquad \pi/2 \tag{12}$$

$$\phi_s(t) = \mathrm{sgn}(x_c)\mathrm{sgn}(\eta) \qquad \pi/2, \tag{13}$$

where the possibilities of negative collimator displacement x_c and negative dispersion η are explicitly taken into account.

B. The grazing function, g

The *grazing angle*—the total angle of a grazing particle—is found by substituting these phases into Eq. (9) and by using Eq. (11) to eliminate a_x. It is

$$x'_G = -\frac{\alpha}{\beta} x_c + \mathrm{sgn}(x_c)\,\mathrm{sgn}(\eta)\left(\frac{\alpha}{\beta}\eta + \eta'\right) a_s. \tag{14}$$

Thus the grazing angle depends linearly on the synchrotron amplitude a_s according to

$$x'_G = -\frac{\alpha}{\beta} x_c + \mathrm{sgn}(x_c)\,\mathrm{sgn}(\eta) g a_s, \tag{15}$$

where the differential of the grazing angle with respect to synchrotron amplitude is

$$\frac{dx'_G}{da_s} = \mathrm{sgn}(x_c)\,\mathrm{sgn}(\eta) g. \tag{16}$$

The dimensionless optical *grazing function* g that enters these equations is defined as

$$g \equiv \left(\frac{\alpha}{\beta}\eta + \eta'\right). \tag{17}$$

Inspection confirms it to be the slope of the normalized dispersion function scaled by the square root of β,

$$g = \sqrt{\beta}\,\eta'_N, \tag{18}$$

where the normalized dispersion is

$$\eta_N = \frac{\eta}{\sqrt{\beta}}. \tag{19}$$

C. A rigorous synchrobetatron condition on g, and its trivial solutions

Any linear dependence of the grazing angle on the synchrotron amplitude is undesirable, since it may cause particles with some synchrotron amplitudes to fall outside the limited angular acceptance of a collimator. The rigorous synchrobetatron condition for constant grazing angle is

$$g = \sqrt{\beta}\,\eta'_N = 0. \tag{20}$$

This is a condition on the optics, independent of the emittance and the energy spread of the beam. Since β is

positive definite, a collimator is ideally placed at a location where normalized dispersion is at a local maximum or minimum. This condition

$$\eta_N' = 0 \tag{21}$$

has already been noted in the literature [1–4]. For example, Bryant and Klein [1] state: When the normalized dispersion has its peak at the primary collimator, all momenta are treated equally [... giving ...] the collimation condition

$$\frac{\eta'}{\eta} = -\frac{\alpha}{\beta} \tag{22}$$

which is almost equivalent to Eq. (20) (except for the factor of $\sqrt{\beta}$). Two particular trivial solutions to the rigorous condition

$$g = \frac{\alpha}{\beta}\eta + \eta' = 0 \tag{23}$$

are immediately obvious: (i) $\eta = \eta' = 0$: anywhere in a dispersion-free straight; (ii) $\alpha = \eta' = 0$: simultaneous extrema of β and η, such as (logically) in the middle of a quadrupole at the boundary of a matched half cell.

General solutions to the rigorous condition can be found at more practical locations in magnet-free straights which are *not* dispersion free. Further, it is sufficient for g to be ''small enough''—complete rigor is not required.

The following sections of this paper go beyond previous work by recognizing that the behavior of g is worth studying in its own right, in much the same ways that the optical functions β and η are studied. The propagation of g through a magnetic lattice is presented next, followed by quantitative discussions of some semiabstract and realistic scenarios, such as the importance of error waves that perturb otherwise perfectly matched periodic optics.

II. GRAZING FUNCTION PROPAGATION

The grazing function is closely related to standard optical functions. Different but equivalent convenient forms include

$$g = b\eta_N' = b\left(\frac{\eta'}{b} - \frac{\eta b'}{b^2}\right) = \left(\eta' - \frac{\eta b'}{b}\right) = \eta\left(\frac{\eta'}{\eta} - \frac{b'}{b}\right), \tag{24}$$

where for simplicity

$$b = \sqrt{\beta}. \tag{25}$$

In all lattice configurations g is readily derived from the optical functions that are numerically generated, element by element, by an optics analysis program such as MAD. This section goes on to consider grazing function propagation in cases of instructive interest, including generic periodic matched optics, dispersion waves, and beta waves. FODO cells are simple examples of particular interest, instructive in terms of approximate quantification and scaling. First, however, some basic intuition is achieved by studying propagation through thin (and short) dipoles and quadrupoles.

A. Propagation through thin dipoles and quadrupoles

The differential equations describing the propagation of dispersion and the horizontal beta function are quite similar to each other:

$$\eta'' + K\eta = \frac{1}{\rho} \tag{26}$$

$$b'' + Kb = b^{-3}. \tag{27}$$

Here K is the geometric strength of the quadrupole field, while ρ is the bending radius of the dipole field. The changes in b' and η' across a *thin dipole* of bend angle $\Delta\theta$ are

$$\Delta\eta' = \Delta\theta \tag{28}$$

$$\Delta b' = 0 \tag{29}$$

while b and η themselves do not change, so that the grazing function has a step of the same size and sign as the bend angle, since

$$\Delta g = \left(\Delta\eta' - \frac{\eta\Delta b'}{b}\right) = \Delta\theta. \tag{30}$$

Similarly, the changes across a *thin quadrupole* of integrated strength $\Delta(KL)$ are

$$\Delta\eta' = -\Delta(KL)\eta \tag{31}$$

$$\Delta b' = -\Delta(KL)b \tag{32}$$

showing that the grazing function is unchanged across a thin quadrupole, since

$$\Delta g = \eta\left(\frac{\Delta\eta'}{\eta} - \frac{\Delta b'}{b}\right) = 0. \tag{33}$$

The top plot in Fig. 1 confirms such propagation of g through thin dipoles and quadrupoles, plotting values of g that were generated by a simple script that reads standard output from an optics analysis code. The bottom plot shows a more realistic situation in which the vanishingly thin magnets have become merely short, while retaining the same integrated strength. In both cases the magnets are arranged in a FODO cell of 50 m total length, with optical functions that obey periodic boundary conditions.

B. Propagation through multiple lattice cells with dispersion waves

Consider a general lattice cell (not necessarily FODO) that is repeated as the lattice is traversed. The optics are *matched* if the dispersion and beta functions obey periodic boundary conditions (PBC) at the end of each cell. The

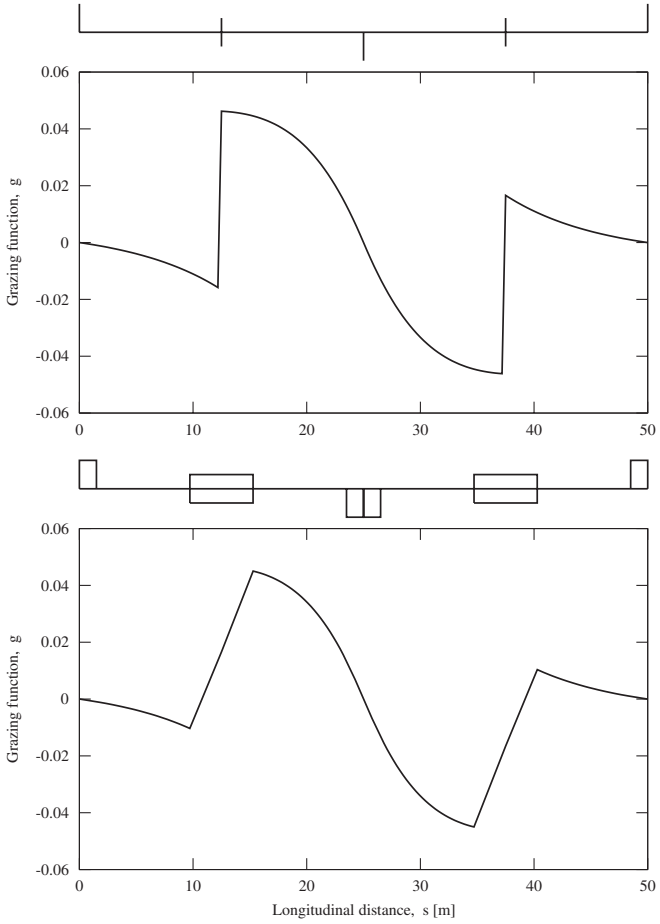

FIG. 1. The grazing function in a matched FODO cell with thin quads and dipoles (top), and partially filled with short quads and dipoles (bottom). In both cases the half cell is $L = 25$ m long, with a phase advance of 90 degrees per full cell in both planes, and with a bend angle of $\theta = \pi/50$ radians per half cell.

actual optics deviate from the matched values—either deliberately or accidentally—by the superposition of dispersion and/or beta waves. Thus,

$$\eta = \eta_P + \eta_W \tag{34}$$

$$\beta = \beta_P + \beta_W, \tag{35}$$

where subscripts P and W denote periodic and wave, respectively. First, consider the case in which there are only dispersion waves (so that $\beta_W = 0$), before returning to consider the opposite case, in which there are only beta waves.

The periodic dispersion is found by solving the differential equation

$$\eta_P'' + K\eta_P = \frac{1}{\rho} \tag{36}$$

with PBC, while the dispersion wave obeys

$$\eta_W'' + K\eta_W = 0 \tag{37}$$

with no boundary conditions. Equation (37) is analogous to the equation for free horizontal betatron oscillations

$$x'' + Kx = 0 \tag{38}$$

indicating that the *exact* solution for dispersion waves is

$$\eta_W = a_\eta\sqrt{\beta}\cos(\phi + \phi_\eta), \tag{39}$$

where the constants a_η and ϕ_η are the amplitude and phase of the dispersion wave.

The exact normalized dispersion in the absence of a beta wave ($\beta = \beta_P$) is

$$\eta_N = \eta_{NP} + a_\eta\cos(\phi + \phi_\eta), \tag{40}$$

where it is convenient to introduce the periodic normalized dispersion

$$\eta_{NP} = \frac{\eta_P}{\sqrt{\beta_P}}. \tag{41}$$

The dependence of the grazing function $g(\phi)$ on the dispersion wave amplitude and phase constants is found by converting the differentiation with respect to s, to differentiation with respect to ϕ, through

$$g = \sqrt{\beta}\frac{d\eta_N}{ds} = \sqrt{\beta}\frac{d\phi}{ds}\frac{d\eta_N}{d\phi} = \frac{1}{\sqrt{\beta}}\frac{d\eta_N}{d\phi} \tag{42}$$

to give *exactly*

$$g = g_P - \frac{a_\eta}{\sqrt{\beta_P}}\sin(\phi + \phi_\eta), \tag{43}$$

where the periodic grazing function is

$$g_P = \frac{1}{\sqrt{\beta_P}}\frac{d\eta_{NP}}{d\phi}. \tag{44}$$

1. The periodic grazing function, $g_P(\phi)$

There is a tendency for the periodic normalized dispersion η_{NP} to be approximately constant. (This is discussed further, below, in the particular case of periodic FODO cells.) Insofar as $d\eta_{NP}/d\phi \approx 0$, then the periodic grazing function $g_P(\phi)$ tends to be small. In the general case of a repetitive cell, without making any assumption about the behavior of the periodic normalized dispersion,

$$g_P(\phi) = \sum_n a_{gn}\sin\left[n2\pi\left(\frac{\phi}{\phi_C}\right) + \phi_{gn}\right], \tag{45}$$

where ϕ_C is the period of the basic cell.

Figure 2 shows 360 degrees of phase advance through matched periodic optics in a set of repetitive FODO cells, each with a total phase advance of 90 degrees, so that

$$\phi_C = 2\pi/4. \tag{46}$$

The beginning of the lattice segment, at $\phi = 0$, is chosen to be at the center of a horizontally focusing quadrupole, so that

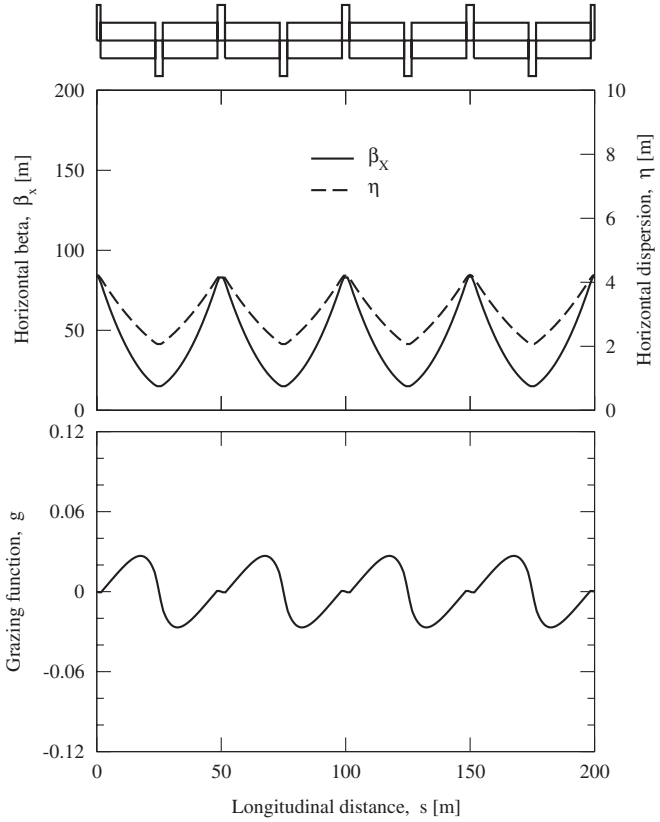

FIG. 2. The matched periodic grazing function g_P in four FODO cells, with a bend angle of $\theta = \pi/50$ per half cell of length $L = 25$ m, and a total phase advance of 360 degrees in both planes. The grazing function is dominated by the 4ϕ harmonic, with a maximum value of 0.0268 that is in good agreement with the thin quadrupole prediction of 0.0260.

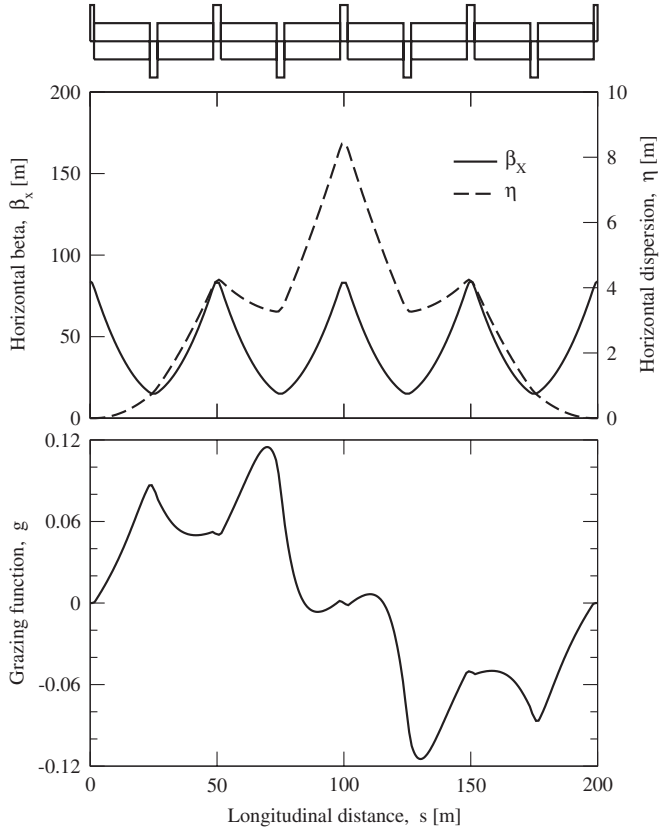

FIG. 3. The grazing function in the presence of a 100% dispersion wave, dominated by the 1ϕ harmonic and modulated by $1/\sqrt{\beta}$, with a maximum g value of 0.115 that is 4 times the maximum in the matched case. The thin quadrupole prediction of 0.0498 at $s = 50$ m agrees well with the actual value of 0.0508.

$$\phi_{gn} = 0 \tag{47}$$

and, simply

$$g_P = \sum_n a_{gn} \sin(4n\phi). \tag{48}$$

The bottom plot in Fig. 2 confirms that the fourth harmonic dominates g_P, and that there are no harmonics except $4\phi, 8\phi, 12\phi, \ldots$ etc. Lower (and potentially stronger) harmonics enter only when dispersion waves or beta waves are present.

2. Dispersion waves, $a_\eta \neq 0$

The exact dependence of the grazing function on phase ϕ in the presence of dispersion waves is found by writing Eq. (43) more fully, as

$$g(\phi) = g_P(\phi) - a_\eta \frac{\sin(\phi + \phi_\eta)}{\sqrt{\beta_P(\phi)}}. \tag{49}$$

Figure 3 shows what happens when a 100% dispersion wave, with amplitude and phase constants

$$a_\eta = \frac{\eta_P(0)}{\sqrt{\beta(0)}} \tag{50}$$

$$\phi_\eta = \pi, \tag{51}$$

is added to the case of repeated FODO cells already illustrated in Fig. 2. In this case

$$g(\phi) = g_P(\phi) + \frac{\eta_P(0)}{\sqrt{\beta_P(0)}} \cdot \frac{\sin(\phi)}{\sqrt{\beta_P(\phi)}}. \tag{52}$$

The bottom plot in Fig. 3 confirms that the first harmonic of ϕ dominates the behavior of g with 100% dispersion waves, modulated by the factor $\sqrt{\beta_P(\phi)}$ in the denominator of Eq. (52). Fourth and eighth order harmonics (etc.) are also present, through the $g_P(\phi)$ term.

C. Propagation through periodic optics with betatron waves

The total β function in the presence of a beta wave of amplitude a_β is given (accurate only *to first order* in a small amplitude $a_\beta \ll 1$) by

$$\beta \approx \beta_P\{1 + a_\beta \cos[2(\phi + \phi_\beta)]\}, \tag{53}$$

where β_P is the periodic matched solution and ϕ_β is the phase of the wave. In the absence of dispersion waves ($\eta = \eta_P$), the normalized dispersion is therefore

$$\eta_N = \frac{\eta}{\sqrt{\beta}} \approx \frac{\eta_P}{\sqrt{\beta_P}}\{1 + a_\beta \cos[2(\phi + \phi_\beta)]\}^{-1/2} \tag{54}$$

or, after expanding the term in curly brackets to first order in a_β,

$$\eta_N \approx \eta_{NP}\left[1 - \frac{a_\beta}{2}\cos[2(\phi + \phi_\beta)]\right]. \tag{55}$$

The total grazing function is given (to first order in a_β) by

$$g(\phi) \approx g_P(\phi) - \frac{a_\beta}{2}\frac{1}{\sqrt{\beta(\phi)}} \cdot \frac{d}{d\phi}\{\eta_{NP}(\phi)\cdot\cos[2(\phi + \phi_\beta)]\}. \tag{56}$$

Using the fact that

$$\frac{d\eta_{NP}}{d\phi} = g_P\sqrt{\beta_P} \tag{57}$$

then, finally

$$g \approx g_P\left[1 - \frac{a_\beta}{2}\sqrt{\frac{\beta_P}{\beta}}\cdot\cos[2(\phi + \phi_\beta)]\right] + a_\beta\frac{\eta_{NP}}{\sqrt{\beta}}\cdot\sin[2(\phi + \phi_\beta)]. \tag{58}$$

Figure 4 shows what happens when a "100%" beta wave, with amplitude and phase constants

$$a_\beta = 1 \tag{59}$$

$$2\phi_\beta = \pi, \tag{60}$$

is added to the same matched periodic FODO optics, so that

$$\beta \approx \beta_P[1 - \cos(2\phi)]. \tag{61}$$

The value of β is halved at $\phi = 0$, but doubled at $2\phi = \pi$ (where $s = 50$ m), confirming that this equation is not a very good approximation with large values of a_β, of order 1. Nonetheless, taking the approximation in Eq. (58) at face value, the grazing function becomes

$$g(\phi) \approx g_P(\phi)\left[1 + \frac{1}{2}\sqrt{\frac{\beta_P}{\beta}}\cdot\cos(2\phi)\right] - \frac{\eta_{NP}}{\sqrt{\beta}}\cdot\sin(2\phi). \tag{62}$$

The bottom plot in Fig. 4 confirms the general features of this approximation. For example, $g(0) = 0$ [in part because $g_P(0) = 0$], and the 2nd harmonic of ϕ dominates g with large beta waves, heavily modulated by the factor of $\sqrt{\beta(\phi)}$ in the denominator. Fourth and higher harmonics are also present, through the presence of $g_P(\phi)$ in the first term of Eq. (62), although the second term clearly dominates.

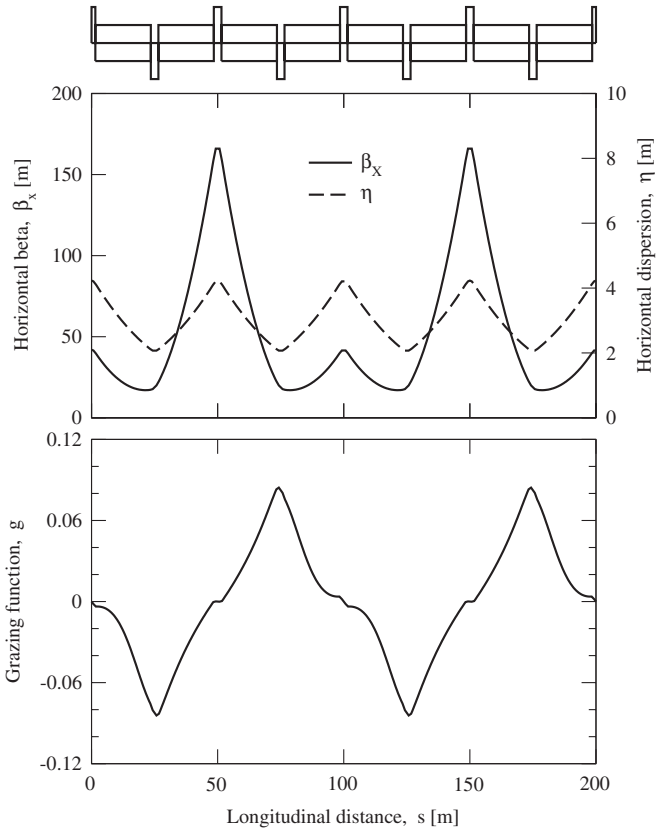

FIG. 4. The grazing function in the presence of a "100%" beta wave, dominated by the 2ϕ harmonic and modulated by $1/\sqrt{\beta}$. The maximum g value of 0.084 is in only fair agreement with the thin quadrupole prediction of 0.139, due to the breakdown of first order perturbation theory with such large perturbations.

D. Quantitative predictions for periodic FODO cells

A case of particular interest—a series of identical FODO cells—is amenable to approximate quantification.

1. Matched FODO cell optics

Consider the case when each *half* cell of length L contains one or more dipoles with a total bend angle of θ, centered halfway along the half cell, with a thin focusing F quadrupole at one end and a D quadrupole at the other. The maximum, minimum, and mid-half-cell beta functions for the matched periodic case are

$$\beta_{PF} = \frac{L}{S}\left(\frac{C}{1-S}\right), \qquad \beta_{PD} = \frac{L}{S}\left(\frac{C}{1+S}\right), \qquad \beta_{PM} = \frac{L}{S}\left(\frac{1+C^2}{2C}\right), \tag{63}$$

where

$$S \equiv \sin(\phi_C/2), \qquad C \equiv \cos(\phi_C/2) \tag{64}$$

and ϕ_C is the phase advance per full FODO cell. The maximum and minimum periodic matched dispersion functions are

$$\eta_{PF} = L\theta\left(\frac{2+S}{2S^2}\right), \qquad \eta_{PD} = L\theta\left(\frac{2-S}{2S^2}\right) \tag{65}$$

so that, although the two extreme normalized dispersions are close in value,

$$\begin{aligned} \eta_{PNF} &= \sqrt{L}\theta\left(\frac{2+S}{2S^{3/2}C^{1/2}}\right)\sqrt{1-S}, \\ \eta_{PND} &= \sqrt{L}\theta\left(\frac{2-S}{2S^{3/2}C^{1/2}}\right)\sqrt{1+S} \end{aligned} \tag{66}$$

nonetheless they differ by a small amount $\Delta\eta_N$. The plausible approximation

$$\eta_N'(s) \approx \frac{\pi}{2}\frac{\Delta\eta_N}{L}\sin\left(\pi\frac{s}{L}\right) \tag{67}$$

(where s is the distance from the beginning of the half cell) ensures that η_N increases by $\Delta\eta_N$ across the half cell, and that η_N' (and hence g) is zero at $s = 0$ and at $s = L$. This is illustrated by Fig. 2 and is indicated by Eq. (48) for a matched periodic cell.

2. Quantitative example of matched FODO cells

The extreme values of η_N' and hence g are expected near the middle of the half cell, at $s = L/2$ where $\beta = \beta_{PM}$. Putting all this together for matched periodic FODO cells with thin quadrupoles and a phase advance per cell of 90 degrees, so that $C = S = 1/\sqrt{2}$, then the maximum of the grazing function is predicted to be

$$g_{P\max} \approx \frac{\pi}{2}\frac{|\Delta\eta_N|}{L}\sqrt{\beta_{PM}} \tag{68}$$

$$\approx \frac{\pi}{4\sqrt{2}}\frac{\sqrt{1+C^2}}{S^2C}[(2-S)\sqrt{1+S} - (2+S)\sqrt{1-S}] \cdot \theta \tag{69}$$

$$\approx 0.41\theta \tag{70}$$

$$\approx 0.0260 \tag{71}$$

with no dependence on the half-cell length L.

Figure 2 confirms that the actual maximum value of g_P occurs close to the mid half cell, with a value of 0.0268 that is surprisingly close to the value of 0.0260 that is predicted by Eq. (70) when $\theta = \pi/50$.

3. Dispersion waves

Figure 3 shows the case of the same periodic FODO cells (with $L = 25$ m) in the presence of a 100% dispersion wave, as described by Eqs. (50)–(52). The grazing function is predicted to have a "typical" value of

$$g_{\text{typ}} = \frac{\eta_{PF}}{\beta_{PF}} \tag{72}$$

$$\approx \left(\frac{2+\frac{1}{\sqrt{2}}}{2+\sqrt{2}}\right)\cdot\theta \tag{73}$$

$$\approx 0.0498 \tag{74}$$

when $\phi = \pi/2$ at $s = 50$ m, in the middle of an F quadrupole, where $g_P = 0$.

The data shown in Fig. 3 have an actual value of $g = 0.0508$ at $s = 50$ m, in good agreement with this prediction. The maximum grazing function has a value of 0.115 at $s = 69.8$ m, more than twice this typical value, largely due to the strong modulation effect caused by the variation of $\sqrt{\beta_P(\phi)}$ in the denominator of Eq. (52). The maximum value of g with a 100% dispersion wave is 4 times the value with perfect matched optics.

4. Beta waves

Figure 4 shows that in the FODO case with no dispersion wave, but with a "100%" beta wave, the maximum value of the grazing function occurs at $s = 75$ m in the center of a D quadrupole, with a value of $g_{\max} = 0.084$.

Equation (62) predicts the maximum grazing function value when $\phi = 3\pi/4$ to be

$$g_{\max} \approx \frac{\eta_{PD}}{\sqrt{\beta_{PD}\beta_D}} \tag{75}$$

if it is naively assumed that $\phi = 3\pi/4$ at 75 m. In fact $\phi = 3\pi/4$ at $s \approx 80.6$ m, due to the presence of a phase wave in quadrature with the beta wave. Nonetheless proceeding to get an order of magnitude estimate for the maximum value, and crudely approximating that

$$\beta_D \approx \beta_{PD} \tag{76}$$

then

$$g_{\max} \approx \frac{\eta_{PD}}{\beta_{PD}} \tag{77}$$

$$\approx \left(\frac{2-\frac{1}{\sqrt{2}}}{2-\sqrt{2}}\right)\cdot\theta \tag{78}$$

$$\approx 0.139. \tag{79}$$

This prediction is 65% larger than the actual value. This discrepancy is not surprising, considering the number of approximations involved in getting to this point.

E. Scaling with angle and length in a matched FODO cell

Numerical testing confirms the prediction of Eq. (69) that the maximum value of the grazing function scales with half-cell length L and with half-cell bending angle θ like

$$g_{P\max} \approx 0.427 L^0 \theta^1 \tag{80}$$

when the phase advance per full cell is 90 degrees in both planes. There is no dependence on the cell length. A fair rule of thumb is that

$$g_{P\max} \approx \theta/2. \tag{81}$$

These two results apply *only* to a matched FODO cell. The grazing function can become much larger in absolute magnitude when a significant unmatched dispersion or betatron wave is present, and in non-FODO locations. In this case Eqs. (73) and (78) similarly predict that

$$g \sim \frac{\eta}{\beta} \sim L^0 \theta^1 \tag{82}$$

with the same scaling.

Finally, insofar as the maximum dispersion function remains remarkably constant at $\eta_{\max} \approx 2$ m over accelerators that span many orders of magnitude of energy E (and ignoring an order of magnitude range of dipole fields), then

$$\theta \sim E^{-1/2} \tag{83}$$

and so also

$$g \sim E^{-1/2}. \tag{84}$$

The grazing function tends to decrease with the square root of the energy.

III. THE GRAZING FUNCTION IN RHIC, SPS, TEVATRON, AND LHC

Table I shows that primary collimators in four hadron colliders—RHIC, SPS, Tevatron, and LHC—have nominal grazing functions in the range from -0.0025 to $+0.0036$, in the absence of optical errors [5–10]. The rigorous condition $g = 0$ has not been attained in these realistic (or proposed) implementations of amorphous and crystal primary collimators. This is in part because ideal locations have not been sought, and in part because they are not available.

Inspection of the pairs of η' and g values in Table I shows that there is a systematically strong cancellation between the two terms $(\alpha/\beta)\eta$ and η' that comprise g in Eq. (17). This reflects the tendency for the normalized dispersion η_N to remain approximately constant in reasonably well-matched optics, so that η'_N and hence g are small.

How small is small enough for the absolute value of the grazing function? How significant are the nonzero g values in Table I?

A. A relaxed grazing function condition for crystal primary collimators

A discussion of implementation-specific details of several collimation systems is beyond the scope of this paper. Nonetheless, a general discussion of the "acceptance angle" σ'_A for protons incident on a crystal primary collimator is possible, even though σ'_A depends strongly on crystal geometry, beam energy, and the mode of operation—channeling or volume reflection. As a rule of thumb the crystal acceptance angle is

$$\sigma'_A[\mu\text{rad}] \sim 4E^{-1/2} \text{ channeling at energy } E[\text{TeV}] \tag{85}$$

$$\sim 100 \text{ volume reflection at any energy.} \tag{86}$$

The volume reflection acceptance angle is simply the crystal bend angle, and so is superficially independent of particle energy. In contrast, the channeling acceptance angle decreases with increasing energy. [Volume reflection therefore appears to become more favored at higher energies, although channeling benefits from the reduction of the grazing function with increasing energy, according to Eq. (84).]

TABLE I. Nominal optics, grazing functions, and other values at primary collimators in four accelerators. The collimator type is recorded as either "A" for amorphous or "C" for crystal. Note that the LHC IR7 location (for betatron cleaning) is almost identical to the tentatively proposed LHC crystal location. The last column records the grazing angle spread across the rf bucket.

	Type	α	β [m]	η [m]	η' [10^{-3}]	g [10^{-3}]	E [TeV]	a_{bucket} [10^{-3}]	σ_p/p [10^{-3}]	σ_x [mm]	$\Delta x'_{TB}$ [μrad]
RHIC	C	−26.5	1155.0	−0.864	−16.2	3.6	0.10	1.50	0.50	7.36	5.40
SPS (UA9)	C	−2.21	96.1	−0.880	−19.0	1.2	0.12	1.10	0.40	1.06	1.32
Tevatron (T-980)	C	−0.425	67.5	1.925	15.0	2.9	0.98	0.45	0.14	0.55	1.31
LHC (IR3)	A	1.72	131.2	2.100	−30.1	−2.5	0.45	0.97	0.31	1.01	2.43
							7.0	0.35	0.11	0.26	0.88
LHC (IR7)	A	2.06	152.0	0.36	−5.6	−0.7	0.45	0.97	0.31	1.09	0.68
							7.0	0.35	0.11	0.28	0.25
LHC (crystal)	C	1.93	136.1	0.341	−5.6	−0.8	0.45	0.97	0.31	1.03	0.78
							7.0	0.35	0.11	0.26	0.28

The crystal acceptance angle can be compared with the grazing angle spread from the center to the edge of the rf bucket (from synchrotron amplitude $a_s = 0$ to $a_s = a_{\text{bucket}}$). The grazing angle spread across the bucket,

$$\Delta x'_{TB} = |g| a_{\text{bucket}}, \tag{87}$$

is especially relevant if a collimator is being used to intercept beam escaping from the rf bucket. The uncaptured beam is a major concern for the Tevatron and the LHC, because such a beam migrates into the abort gap and can quench superconducting magnets—or even do irreversible damage—during an emergency abort [11]. Abort gap beam is heated transversely in the Tevatron to large a_x by a time-gated electron lens. The T-980 crystal collimation experiment is being used (in part) to study this beam. The LHC will probably also transversely heat abort gap beam.

The grazing angle spread across the bucket is recorded in the last column of Table I. In general (avoiding scenario-specific details) it is desirable for this spread to be much less than the collimator acceptance angle,

$$\Delta x'_{TB} \ll \sigma'_A. \tag{88}$$

Thus the relaxed condition on the grazing function for efficient collimation is

$$|g| \ll \frac{\sigma'_A}{a_{\text{bucket}}}. \tag{89}$$

B. How significant are actual g values?

Figure 5 shows how the grazing angle spread across the rf bucket $\Delta x'_{TB}$ compares with the (approximate) channeling acceptance angle σ'_A given in Eq. (85), across 2 orders of magnitude in beam energy E. Both amorphous and crystal primary collimator locations are shown, with different symbols. The grazing function values g lead to total angular spreads that are "safe" in all cases for nominal optics without errors, but by as little as a factor of 2. As expected, the grazing angle spread across the rf bucket decreases (approximately) with the square root of energy E.

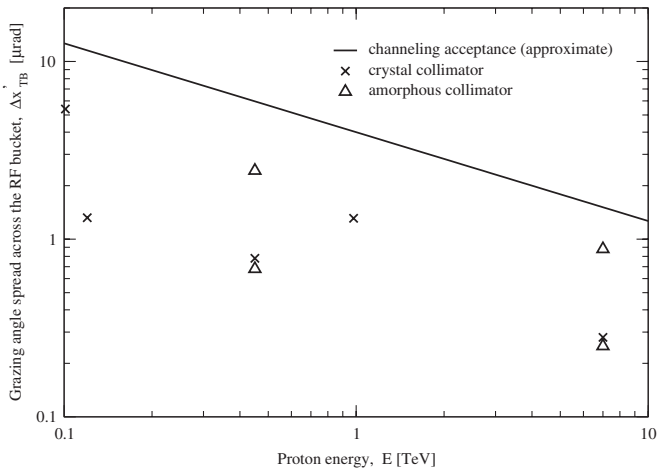

FIG. 5. Variation of the grazing angle spread across the rf bucket as a function of energy for amorphous and crystal primary collimators according to the data in Table I for RHIC, SPS, Tevatron, and LHC. The solid line maximum limit follows the inverse square root rule of thumb given by Eq. (85) for the primary collimator acceptance angle under crystal channeling. The grazing angle spreads appear to relatively safe, at least for nominal design optics without errors.

IV. SUMMARY

The *grazing function* g parametrizes the rate of change of total angle with synchrotron amplitude for grazing particles—those that just touch the surface of a collimator or other aperture when their synchrotron and betatron oscillations are simultaneously (in time) at their extreme displacements. The grazing function is a pure optics function, closely related to the slope of the normalized dispersion function. It can depend strongly on the azimuthal location of the collimator (but does not depend on the type of collimator). It has an ideal value of $g = 0$ at the collimator.

The grazing function is naturally small in well-matched optics with no (or small) dispersion and betatron waves. Although g is identically zero across a dispersion-free straight, it is not in general necessary to make dispersion (and the dispersion slope) zero at the collimator. Most important is the need to eliminate significant betatron and dispersion waves (in design and in error), since they can increase g by half an order of magnitude.

Insofar as g is nonzero in practical implementations (for example, due to optics errors or to external design constraints), then nonetheless it should be kept small enough in magnitude so that all particles over the relevant synchrotron amplitude range (for example, across an rf bucket) remain within the collimator acceptance angle. This appears to be reasonable to achieve in practice with crystal collimators, especially when they are operating in volume reflection mode, but also when in channeling mode.

Design values for past, present, and future crystal implementations in RHIC, SPS, Tevatron, and LHC suggest that the nominal realistic values of g are acceptably small, although they are not negligible. Planning for future crystal implementations should always include a grazing function analysis, both in design (making g zero, or small enough) and in error analysis (ensuring that g cannot become anomalously large).

ACKNOWLEDGMENTS

We would like to thank Ralph Assmann, Angelika Drees, Ray Fliller, Jean-Bernard Jeanneret, Emanuele Laface, Nikolai Mokhov, Eric Prebys, Guillaume Robert-Demolaize, Walter Scandale, Dean Still, and Alexander

Valishev, for their help and encouragement. One of us (Peggs) would like to send special thanks to LARP and (in particular) to Tom Markiewicz, for their long suffering support and forbearance. Without them this paper would not have been possible.

[1] P. Bryant and E. Klein, CERN Report No. CERN-SL/92-40, 1992.
[2] M. Seidel, DESY Report No. DESY-94-103, 1994.
[3] T. Trenkler and J.-B. Jeanneret, Part. Accel. **50**, 287 (1995).
[4] J.-B. Jeanneret, Phys. Rev. ST Accel. Beams **1**, 081001 (1998).
[5] R. P. Fliller, Ph.D. thesis, Stony Brook University [Report No. UMI-31-61096, 2004].
[6] R. P. Fliller *et al.*, Phys. Rev. ST Accel. Beams **9**, 013501 (2006).
[7] A. Drees and R. Fliller (private communication).
[8] E. Laface (private communication).
[9] D. Still and A. Valishev (private communication).
[10] C. Bracco, Ph.D. thesis, EPFL, Lausanne, 2008.
[11] E. Shaposhnikova, S. Fartoukh, and J.-B. Jeanneret, in *Proceedings of the 9th European Particle Accelerator Conference, Lucerne, 2004* (EPS-AG, Lucerne, 2004), MOPLT031, p. 661.